

See discussions, stats, and author profiles for this publication at: <https://www.researchgate.net/publication/277783056>

Back Cover: Switch-On Fluorescence of a Perylene-Dye-Functionalized Metal-Organic Framework through Postsynthetic Modification (Chem. Eur. J. 30/2015)

ARTICLE in CHEMISTRY - A EUROPEAN JOURNAL · JUNE 2015

Impact Factor: 5.73 · DOI: 10.1002/chem.201406157 · Source: PubMed

READS

38

6 AUTHORS, INCLUDING:



Jörn Schmedt auf der Günne

Universität Siegen

68 PUBLICATIONS 1,233 CITATIONS

SEE PROFILE



Stefan Wuttke

Ludwig-Maximilians-University of Munich

44 PUBLICATIONS 813 CITATIONS

SEE PROFILE

Metal-Organic Frameworks



Switch-On Fluorescence of a Perylene-Dye-Functionalized Metal-Organic Framework through Postsynthetic Modification

Christian Dietl,^[a] Henrik Hintz,^[a] Bastian Rühle,^[a] Jörn Schmedt auf der Günne,^[b] Heinz Langhals,^{*[a]} and Stefan Wuttke^{*[a]}

Abstract: A perylene dye was introduced directly as a linker into a metal-organic framework (MOF) during synthesis. Depending on the dye concentration in the MOF synthesis mixture, different fluorescent materials were generated. The successful incorporation of the dye was proven by using ¹³C and ²⁷Al MAS NMR spectroscopy, by solution NMR spectroscopy after digestion of the MOF sample, and by synthesizing a reference dye without connecting groups, which could coordinate on the metal-oxo cluster inside the MOF. Fluores-

cence quenching effects of the MOF linker, 2-aminoterephthalate, were observed and overcome by postsynthetic modification with acetic anhydride. We show here for the first time that amino groups, which can be used as anchoring points for covalent attachment of other molecules, are responsible for fluorescence quenching. Thus, a very promising strategy to implement switchable fluorescence into MOFs is shown here.

Introduction

Metal-organic frameworks (MOFs) are crystalline materials that have attracted considerable attention in recent years. They feature an extremely high porosity, a huge structural variety and flexibility, as well as high degree of tailorability. Because of these properties they have potential applications in many areas including gas storage, separation, catalysis, and even in biomedicine.^[1–3] Another possible application of MOF materials is the design of MOF chemosensors, which need the implementation of a receptor and a transducer mode.^[4] Following the definition given by the International Union of Pure and Applied Chemistry (IUPAC), a chemical sensor is a device that transforms chemical information into an analytically useful signal.^[5] Therefore, a molecular recognition process is necessary that selectively interacts (usually noncovalent) with the analyte (receptor mode). Furthermore, the system must incorporate a mechanism that can report this binding event to the macroscopic world (transducer mode). There are several analytical techniques for reporting the molecular recognition event, be it qualitatively or quantitatively. Among the different chemi-

cal sensors, luminescent-based ones possess many advantages: Luminescence measurements are usually very sensitive and they can easily be performed, offering high spatial resolution and low cost.^[6] Therefore, it is not surprising that luminescence labelling of MOFs is becoming more and more important for the synthesis of MOF chemosensors.^[4]

To introduce luminescence into the MOF scaffold several methodologies have been developed.^[7] Besides luminescence from the MOF metal center,^[4,7–9] one important strategy is to connect a functionalized dye in a postsynthetic reaction with the MOF linker^[10–13] or with the metal center.^[13] Furthermore, there are examples demonstrating that a chromophore can be used as a MOF linker.^[15–17] In contrast to that, in this article we report for the first time on the use of prefunctionalized dye-linker molecules that can be incorporated as a doping fraction into a MOF (Figure 1). The general feasibility of this so-called mix-linker or mix-and-match approach was already shown by the groups of Yaghi, Lin, and Baiker.^[18–21] By using this strategy, the dye can be attached to the linker molecule without losing its spectroscopic properties. During the MOF synthesis the dye-linker should meet several criteria: 1) Solubility has to be sufficient to achieve incorporation; 2) The thermostability of the dye-linker must be compatible with the synthesis temperature of the MOF; and 3) The steric demand of the dye-linker has to match the pore size of the MOF. Moreover, an important challenge after incorporation of a fluorescence dye molecule inside the MOF structure is the possibility of luminescence quenching.^[14,22] Quenching of an incorporated dye into the porous MOF scaffold could be caused by interaction of the dye with the metal centers, with the aromatic groups, or with functional groups of the organic linker. In addition, concentration- or self-quenching-effects of the dye itself could also be an issue. Despite the necessity of understanding and avoiding this

[a] Dr. C. Dietl, H. Hintz, Dr. B. Rühle, Prof. Dr. H. Langhals, Dr. S. Wuttke
Department of Chemistry and Center for NanoScience (CeNS)
University of Munich (LMU), Butenandtstrasse 11 (E), 81377 München (Germany)
E-mail: Langhals@lrz.uni-muenchen.de
stefan.wuttke@cup.uni-muenchen.de

[b] Prof. Dr. J. Schmedt auf der Günne
Department of Chemistry/Biology, University of Siegen
Adolf-Reichwein-Straße 2, 57076 Siegen (Germany)

Supporting information for this article is available on the WWW under
<http://dx.doi.org/10.1002/chem.201406157>.

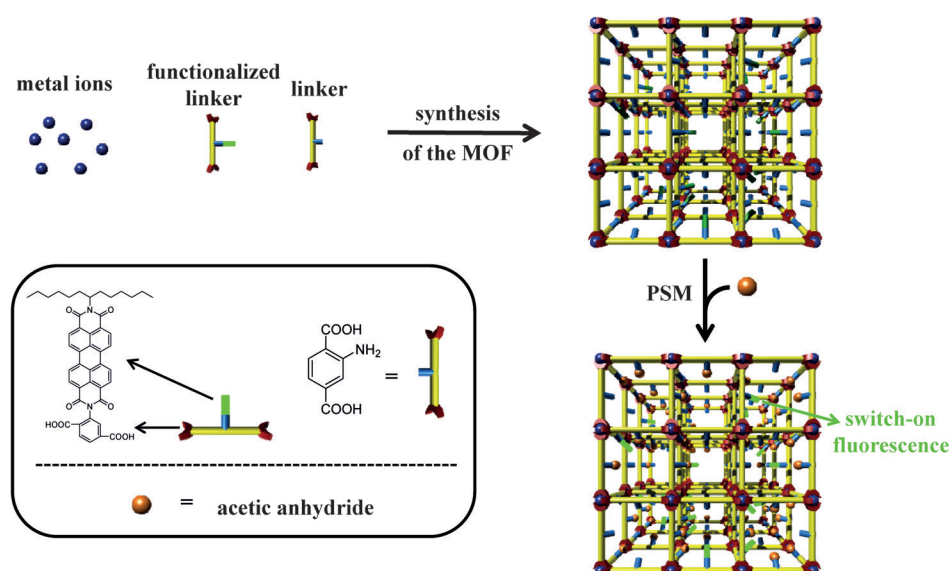


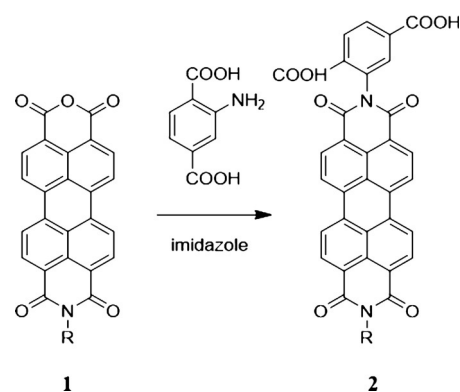
Figure 1. Schematic illustration of the synthesis of a dye-functionalized MOF by using the amino-functionalized linker and a small amount of prefunctionalized dye-linker. In a second step, the fluorescence of the dye can be switched on by post-synthetic modification (PSM) of the MOF structure.

quenching effect, there is little knowledge available about this particular problem in literature so far.^[4]

In the present work we report on the synthesis of perylene-dye-functionalized MIL-101(Al)-NH₂ MOF by using a perylene-functionalized linker as a doping fraction in the MOF synthesis (Figure 1). MIL-101(Al)-NH₂ (with the empirical formula [Al₃OCl(H₂O)₂(bdc-NH₂)₃]) (bdc-NH₂ = 2-amino-1,4-benzenedicarboxylate) contains two types of cages with 29 and 34 Å internal free diameter accessible through pentagonal (12 Å diameter) and hexagonal windows (16 Å diameter).^[23–25] Therefore, this structure can host large molecules and the successful covalent incorporation of drugs and biomolecules could recently be demonstrated.^[26] For the incorporation of a fluorescence dye we chose a perylene dye because it features high chemical stability, light-fastness, high fluorescence quantum yield close to unity, and high molar absorptivities.^[27,28] The amount of incorporated perylene-functionalized linkers can be varied over a wide range, resulting in porous materials with different color intensity (the Supporting Information, Figures S6, S13, and S14). Surprisingly, the fluorescence of the perylene dye is totally suppressed after incorporation into MIL-101(Al)-NH₂, although Al^{III} ions are considered as non-quenching, coordinatively unsaturated metal sites because they have no relevant d–d transition. However, the fluorescence could be switched on by acetylation of the remaining amino groups (Figure 1), which proves that those are the origin of fluorescence extinction. We believe that all these findings can help in the future to synthesize a MOF optical chemosensor.

Results and Discussion

For the preparation of a dye-functionalized linker, perylene-3,4:9,10-tetracarboxylic diimides were chosen because of their unusually valuable properties such as high fluorescence quantum yield and thermal, chemical, and photochemical persistence.



Scheme 1. Synthesis of the perylene bisimide **2** linker. R = 1-hexylheptyl.

tendency to form micelles in alkaline solution. The best results were obtained by keeping the medium strongly acidic during all steps of the reaction, which suppresses the surface-active properties. The commonly applied extraction of the crude reaction mixture with alcohol should be omitted for **2**, because this may cause an acid-catalyzed partial esterification. The last concern is that the perylene bisimide linker **2** matches the pore size of the MIL-101(Al)-NH₂ structure. However, with a maximal projection diameter of 23.2 Å the perylene bisimide linker **2** can easily fit inside both cages of MIL-101(Al)-NH₂ with 29 and 34 Å internal free diameter (the Supporting Information, Figure S5).

The reaction conditions used for the preparation of MIL-101(Al)-NH₂^[24] were applied without any modifications except for the addition of a slight amount of perylene **2**. One significant advantage of this method is that the composition of the final MOF can easily be controlled by varying the amount of prefunctionalized dye-linker. The synthesis of several MOF-dye hybrid materials with an initial molar ratio of 2-aminoterephthalic acid and dye-functionalized linker **2** of 40:1, 200:1,

cy.^[29,30] Long-chain secondary alkyl groups (“swallow-tail” substituents) guarantee good solubility in organic solvents. We started the synthesis of dye **2** with the condensation of 2-aminoterephthalic acid, the linker molecule used in MIL-101(Al)-NH₂ synthesis, with the mono imide mono anhydride **1**, see Scheme 1 (for synthetic details see the Experimental Section). Good results have been obtained with mild reaction conditions for the condensation in molten imidazole.^[31] The work-up of the reaction mixture needs to be adapted to the special properties of **2** concerning the strong detergent properties and

1100:1 (named as MIL-101(Al)-NH₂-perylene40, MIL-101(Al)-NH₂-perylene200, and MIL-101(Al)-NH₂-perylene1100, respectively), or even more diluted, was successful. The obtained red powders were purified by heating at reflux in ethanol and by Soxhlet extraction in chloroform to remove residues of solvent, linker, and dye-linker (for details, see the Experimental Section).

Powder X-ray diffraction (PXRD) measurements of the MIL-101(Al)-NH₂ MOF material, as well as the dye-functionalized ones are in good agreement with each other and the predicted patterns from the literature,^[23,24] indicating that the crystalline structure remains intact upon incorporation of dye **2** (the Supporting Information, Figure S7). The sorption isotherms of perylene-functionalized MIL-101(Al)-NH₂ adducts illustrate a decrease in the surface area and total pore volume in comparison to the unfunctionalized material, which indicates the successful incorporation of the perylene linker **2** (the Supporting Information, Figures S8 and S9). The color intensities of the different materials (Figure 2 and the Supporting Information, Figure S6) increase with increasing amount of linker-dye **2**, which suggests a higher incorporation of this linker. This assumption is supported by the successive decrease of the surface area and total pore volume (the Supporting Information, Figures S8 and S9). However, the proof of incorporation of the functionalized linker in the MOF structure is in general a critical issue when using this mix-linker approach.^[18–21] To prove the incorporation of the perylene linker **2** into the MIL-101(Al)-NH₂ scaffold, different experiments were conducted.

The MIL-101(Al)-NH₂-perylene40 sample was digested and analyzed by using NMR spectroscopy, see Figure S8 (the Supporting Information). In the crude digested mixture, dye **2** and 2-aminoterephthalic acid were identified. The sample was purified by column chromatography to remove the 2-aminoterephthalic acid and unchanged dye **2** was clearly detectable in the eluate (the Supporting Information, Figure S10). Further proof for the successful incorporation of dye **2** inside the MIL-101(Al)-NH₂ structure can be obtained from solid-state MAS NMR spectroscopy. Recently, this technique has even been used for the generation of three-dimensional (3D) maps from multivariate metal-organic frameworks (MTV-MOFs).^[32] We compared the ²⁷Al MQMAS spectra of the unfunctionalized MOF and the dye-functionalized MIL-101(Al)-NH₂-perylene40 (Figure 2). For the dye-functionalized MOF we expect a resonance that shows inhomogeneous broadening due to the disorder introduced by the linker-dye molecules. This effect can be observed for the ²⁷Al NMR spectroscopic resonance at $\delta = 3\text{--}4$ ppm (Figure 2), for which filling the pores with dye molecules that are bound to the linker molecules leads to a further broadening of the signal. Also, the observed peak with a chemical shift of $\delta = 3\text{--}4$ ppm is in perfect agreement with ²⁷Al multiple-quantum magic-angle spinning (MQMAS) of the unfunctionalized MOF structure. The ¹³C NMR spectra give evidence of the organic components in the sample, namely, the linker molecules (2-aminoterephthalic acid), the dye-linker **2**, and the organic solvent molecules in the pores. The ¹³C MAS NMR spectrum of the functionalized MOF can be understood as a superposition of the spectra of the individual components (Figure 2). The spinning sidebands observed for the resonances belonging to the dye molecules are indicative of a constrained motional process, as expected for dye molecules chemically bound to a linker molecule of the MOF structure. For dye molecules moving randomly in solution, no spinning sidebands are expected. Thus the NMR experiments support the hypothesis that perylene linker **2** is incorporated in the MIL-101(Al)-NH₂ scaffold. Last but not least, to confirm that the perylene linker **2** is coordinating Al^{III} ions with its carboxylic acid groups, a reference dye **3** with only a phenyl ring was synthesized and used under the same reaction conditions. After the washing steps, the yellow product showed no evidence of any dye incorporation. PXRD confirms the MIL-101(Al)-NH₂ structure and BET surface area suggest the unfunctionalized MOF structure (the Supporting Information, Figures S7–S9). Hence, the carboxylic acid moieties are essential for the formation of the dye-functionalized MOF materials. In conclusion, all results suggest the incorporation of perylene linker **2** into the MIL-101(Al)-NH₂ structure.

Interestingly none of the prepared MOF-dye materials exhibit solid state fluorescence. Quenching effects of the metal centers can be excluded, because of the lack of occupied d-orbitals of Al^{III} ions and the absence of redox chemistry of the metal. Therefore, the amino groups of the 2-aminoterephthalic acid linker are considered to be responsible for the fluorescence extinction. The lone pair of the amino functionality can lead to the deactivation of the excited states of the chromophores. This single electron transfer (SET) mechanism is well

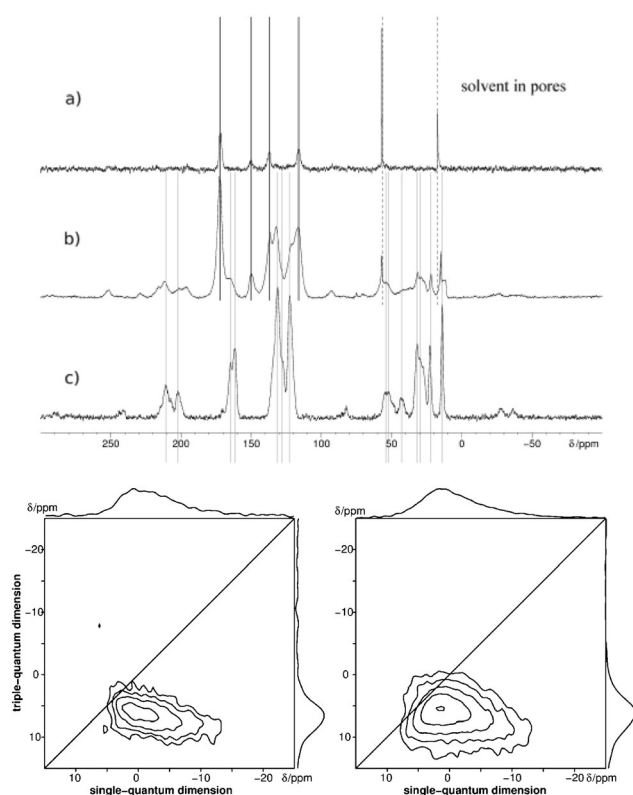


Figure 2. Top: Solid-state ¹³C{¹H} CP MAS NMR spectra. a) MIL-101(Al)-NH₂; b) MIL-101(Al)-NH₂-perylene40; c) dye **2**. Bottom: Solid state ²⁷Al MQMAS spectra of MIL-101(Al)-NH₂ (left) and MIL-101(Al)-NH₂-perylene40 (right).

known for perylene diimides.^[33] To switch-on the fluorescence, the energy of the n-orbitals has to be reduced. Decreasing the energy of these orbitals below the HOMO of the chromophores should suppress these effects, see Figure 3.^[33]

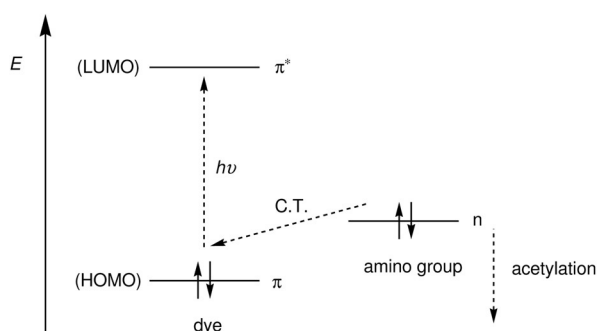


Figure 3. Schematic representation of the energy levels of the HOMO and the LUMO of the perylene chromophore (C.T.: charge transfer). Acetylation of the amino groups lowers the n-orbitals.

A postsynthetic modification (PSM) of the amino groups could be a way to lower the energy of the n-orbitals. Several reactions to modify an amino group were established and applied on different types of amino-tagged MOFs.^[34] Instead of using mixtures of solvents with acetic anhydride, the MOF was treated with pure acetic anhydride for 10 min at 100 °C.^[35] A degradation of the MOF scaffold was neither observed by XRD measurements, see Figure S7 (the Supporting Information), nor visible during the reaction. Even a small degree of decomposition would have led to a release of dye **2**, which is rather soluble in acetic anhydride and would have been easily detected due to the very high extinction coefficient of the dye. Moreover, the samples show the normal decrease in BET surface area after covalent attachment of molecules to the MOF linker (the Supporting Information, Figures S8 and S9).^[34] The PSM yields and consequently also the proof of covalent attachment of acetic anhydride were obtained from ¹H NMR spectra after sample digestion (the Supporting Information, Figure S11).

Solid state fluorescence measurements showed that all acetylated MOFs exhibit strong fluorescence (Figure 4). Therefore, it was possible to lower the energy of n-orbitals by acetylation, avoiding charge transfers, and consequently switch on the fluorescence of the incorporated dye **2**.

The fluorescence spectra according to Figure 4 are typical for the progressive aggregation of perylene dyes with increasing concentration. The spectrum obtained at low concentration of dye (red line) resembles the fluorescence spectrum of the isolated terephthalic-based chromophore in chloroform (black line), in which vibronic structures can still be seen. The spectrum gets more bathochromic components with increasing concentration (green line) and, finally, appears bathochromically shifted (blue line). Both the bathochromic shift and the altered spectral structure are typical for aggregated dyes or dyes in close proximity.^[36] The aggregated dye can be simulated by means of cyclophane^[37] as a model for a permanent H-type aggregate in which a similar bathochromic shift and

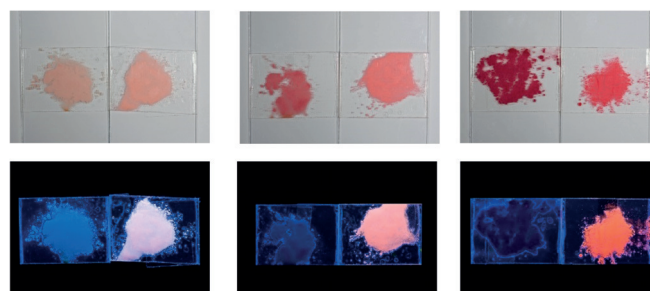
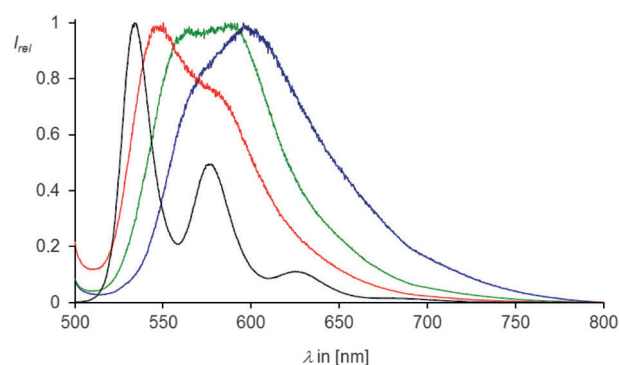


Figure 4. Top: Solid-state fluorescence (excitation $\lambda_{\text{exc}}=490$ nm) spectra of acetylated MOF-dye derivatives (MIL-101(AI)-NH₂-perylene1100Post (red line), MIL-101(AI)-NH₂-perylene200Post (green line), MIL-101(AI)-NH₂-perylene40-Post (blue line)) compared to the fluorescence spectrum of perylene bisimide **2** linker (black) in CHCl₃. Bottom: Photographs of MOF-samples at ambient light (top) and at 366 nm radiation (bottom). From left to the right: MIL-101(AI)-NH₂-perylene1100 and MIL-101(AI)-NH₂-perylene1100Post, MIL-101(AI)-NH₂-perylene200 and MIL-101(AI)-NH₂-perylene200Post, MIL-101(AI)-NH₂-perylene40 and MIL-101(AI)-NH₂-perylene40Post.

spectral structure can be observed (see Figure S12, the Supporting Information). As a consequence, isolated chromophores seem to be preferentially incorporated at low concentration, whereas more and more dyes are interacting with each other at higher concentrations.

Conclusion

In this report, we have demonstrated that the linker-containing perylene dye can be used as a small doping fraction for the synthesis of fluorescent MIL-101(AI)-NH₂ material. The integration of the functionalized linker into the MOF structure could be proven by different techniques. Therefore, this work is an important contribution to assemble structures from linkers with different functional groups, in our case perylene bisimide linker **2** and 2-aminoterephthalic acid, but with an unchanged length of the linker and consequently unaltered connectivity. Importantly, this powerful functionalization approach was used for the first time to introduce a sophisticated linker with a specific property. Although the incorporation of the dye linker inside the MOF scaffold was successful, the material initially does not exhibit any fluorescence. This quenching effect cannot be explained by the presence of metal sites but rather by the functional amino groups. The fluorescence can be switched-on by postsynthetic modification of these groups. Depending on the concentration of the incorporated dye, dif-

ferent fluorescence emission spectra could be observed due to isolated chromophores at low concentration and chromophores in close proximity at higher concentrations.

At this point it shall be highlighted that the method that we used to incorporate a fluorescent dye inside a MOF scaffold can be transferred to any other fluorescent dye that possesses the right thermostability and solubility for the MOF synthesis. The concentration of the dye can easily be lowered to prevent any self-quenching. Because the fluorescence can be switched-on by the covalent attachment of an electron acceptor to the amino group, this step could be used to incorporate the receptor. Hence, this promising strategy could be used in the future for the fabrication of a selective recognition MOF chemosensor.

Experimental Section

Materials

Acetic anhydride (p.A.), acetic acid (in-house chemical supply), aluminium(III) chloride hexahydrate (99.9%, Aldrich), 2-amino terephthalic acid (99%, Aldrich), *N,N*-dimethylformamide (99.8%, Aldrich), hydrochloric acid (in-house chemical supply), formamide (99%, Aldrich), caesium fluoride ($\geq 98.0\%$, Aldrich), chloroform (in-house chemical supply), deuterium oxide (99.9%, Eurisotop), $[D_6]$ dimethylsulfoxide (99.8%, Eurisotop), ethanol (for analysis, in-house chemical supply), imidazole (99%, Aldrich), perylene mono imide mono anhydride **1**.^[37]

Characterization

Nitrogen sorption: Nitrogen sorption measurements were performed on a Quantachrome NOVA 4000e station at 77 K. Outgassing of 20–30 mg sample was performed for 12 h at 423 K. Scientific evaluation of sorption data was carried out with the software suite NovaWin, Version 10.0 (Quantachrome Instruments 2007). BET surface areas for all samples were calculated employing the linearized form of the BET equation with 6 data points ($p/p_0 = 0.050, 0.075, 0.100, 0.125, 0.150, \text{ and } 0.200$) in the range from p/p_0 0.05 to 0.2. For all samples the correlation coefficient was higher than 0.999.

X-ray Diffraction (XRD): Powder X-ray diffraction (PXRD) measurements were performed by using a Bruker D8 diffractometer ($Cu_{K\alpha 1} = 1.5406 \text{ \AA}$; $Cu_{K\alpha 2} = 1.5444 \text{ \AA}$) in θ – θ geometry equipped with a Lynx-Eye detector. The powder samples were measured between 2 and $20^\circ 2\theta$, with a step-size of $0.05^\circ 2\theta$.

NMR spectroscopy: Analyses were performed on a Bruker AMX 600 (Varian Vnmrs 600) or JEOL ECX-400. For the deuterium lock chloroform and $[D_6]$ DMSO were used as an internal reference.

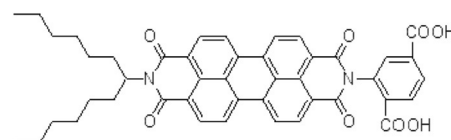
Solid-state nuclear magnetic resonance: The NMR experiments were carried out on a BRUKER Avance III 500 spectrometer equipped with a commercial 4 mm MAS NMR probe. The magnetic field strength was 11.75 T corresponding to ^{13}C and ^{27}Al resonance frequencies of 125.8 and 130.5 MHz, respectively. The deshielding values reported for ^{13}C and ^{27}Al refer to 1% $\text{Si}(\text{CH}_3)_4$ in CDCl_3 and a solution of $\text{Al}(\text{NO}_3)_3$ 1.1 mol kg^{-1} in D_2O . The ^1H resonance of 1% $\text{Si}(\text{CH}_3)_4$ in CDCl_3 served as an external secondary reference using the Ξ value for ^{27}Al as reported by IUPAC.^[37] Saturation combs were applied prior to all repetition delays. A triple-quantum ^{27}Al MQMAS 2D spectrum was acquired using a three-pulse sequence with a zero-quantum filter,^[39] a repetition delay of 10 s and rotor-

synchronized sampling of the indirect dimension. Phase cycling involved the States method for acquisition of pure absorption line shapes and a 48 step phase cycle for coherence transfer pathway selection. The SOQE parameters and isotropic chemical shift values were determined by momenta analyses^[39,40] from the extracted rows of the sheared MQMAS spectrum. The ^{13}C MAS NMR spectra were obtained with a ramped $^{13}\text{C}\{^1\text{H}\}$ cross-polarization experiment at contact time of 5 ms and a sample spinning frequency of 10 kHz.

Solid-state fluorescence: The experiments were run on a Varian Cary Eclipse (detector Hamamatsu R3896, excitation slit 5.0 nm, emission slit 5.0 nm, data interval 0.20 nm, averaging time 0.10 s, detector voltage 590 mV, scan rate 120 nm min^{-1}) equipped with a solid sample holder. About 1 mg of the corresponding sample were spread between two glass slides and fixed on the sample holder.

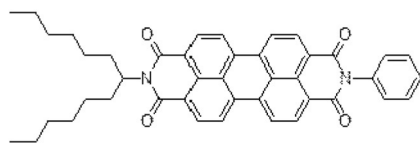
Sample preparation

2-[9-(1-Hexylheptyl)-1,3,8,10-tetraoxo-3,8,9,10-tetrahydro-1H-anthra[2,1,9-def;6,5,10-d'e'f]diisoquinolin-2-yl]terephthalic acid



(**2**): 9-(1-Hexylheptyl)-2-benzopyrano[6',5',4':10,5,6]anthra[2,1,9-def]isoquinoline-1,3,8,10-tetraone (200 mg, 0.35 mmol)^[37] and 2-amino-terephthalic acid (190 mg, 1.1 mmol) were dissolved in molten imidazole (1.5 g) at 140°C and stirred for 2 h. The mixture was dissolved in CHCl_3 and washed with aqueous HCl (2 M, $2 \times 100 \text{ mL}$). The organic phase was collected, washed with distilled water, dried with Na_2SO_4 , and evaporated in vacuo. The residue was purified by using column separation (silica gel $800 \times 44 \text{ mm}$, chloroform/acetic acid 20:1). The residue was dissolved in a minimum amount of a mixture of CHCl_3 and acetic acid, an excess of distilled water was added and the CHCl_3 was removed completely in vacuo. The solid was collected by vacuum filtration (D4 glass filter) and dried at 110°C . Yield: 170 mg (64%), red solid, M.p. $> 250^\circ\text{C}$. R_f value (silica gel, chloroform/acetic acid 20:1): 0.30. ^1H NMR (600 MHz, $\text{CDCl}_3/(\text{CD}_3)_2\text{SO}$ (10:1), 25°C): $\delta = 0.77$ (t, $^3J(\text{H,H}) = 6.9 \text{ Hz}$, 6H, $2 \times \text{CH}_3$), 1.23–1.32 (m, 16H, $8 \times \text{CH}_2$), 1.77–1.84 (m, 2H, $\beta\text{-CH}_2$), 2.15–2.23 (m, 2H, $\beta\text{-CH}_2$), 5.10–5.16 (m, 1H, N-CH), 8.00 (d, $^4J(\text{H,H}) = 1.7 \text{ Hz}$, 1H, CH_{aryl}), 8.18 (dd, $^3J(\text{H,H}) = 8.2$, $^4J(\text{H,H}) = 1.7 \text{ Hz}$, 1H, CH_{aryl}), 8.28 (d, $^3J(\text{H,H}) = 8.2 \text{ Hz}$, 1H, CH_{aryl}), 8.56–8.64 ppm (m, 8H, $8 \times \text{CH}_{\text{perylene}}$); ^{13}C NMR (100 MHz, $\text{CDCl}_3/(\text{CD}_3)_2\text{SO}$ (10:1), 25°C): $\delta = 14.0, 22.5, 26.9, 31.7, 32.3, 54.7, 123.0, 123.2, 123.4, 126.4, 126.7, 129.5, 130.0, 130.2, 131.6, 131.9, 132.2, 132.5, 134.9, 135.6, 135.9, 163.5, 165.8, 166.8 \text{ ppm}$; IR (ATR): $\tilde{\nu} = 2952.5$ (w), 2924.2 (m), 2855.5 (w), 1711.4 (w), 1695.0 (s), 1652.1 (m), 1592.1 (s), 1575.8 (m), 1504.7 (w), 1456.0 (w), 1432.5 (m), 1432.5 (m), 1341.4 (s), 1303.0 (w), 1252.7 (m), 1199.8 (w), 1175.6 (w), 1124.9 (w), 1108.1 (w), 966.5 (m), 854.0 (m), 808.5 (s), 743.3 (s), 658.6 cm^{-1} (m); UV/Vis (CHCl_3): λ_{max} (E_{rel}) = 459.8 (0.22), 490.2 (0.62), 527.0 nm (1.00); Fluorescence (CHCl_3 , $\lambda_{\text{exc}} = 490 \text{ nm}$): λ_{max} (I_{rel}) = 534.6 (1.00), 576.0 (0.53), 626.4 nm (0.12); Fluorescence quantum yield (CHCl_3 , $\lambda_{\text{exc}} = 490 \text{ nm}$, $E_{490 \text{ nm}/1 \text{ cm}} = 0.0152$, reference 2,9-bis-(1-hexylheptyl)anthra[2,1,9-def;6,5,10-d'e'f]diisoquinoline-1,3,8,10(2H,9H)-tetraone RN110590-84-6 with $\Phi = 1.00$): 0.90; MS (FAB⁺): m/z (%): 737.5 (22) [$M^+ + \text{H}$], 719.4 (41), 555.3 (100), 537.3 (68), 509.3 (57), 391.2 (40); HRMS: m/z calcd (%) for

$C_{45}H_{40}N_2O_8$: 737.2863 [$M^+ + H$]; found: 737.2852 [$M^+ + H$], $\Delta = -0.0011$.



(1-Hexylheptyl)-9-phenylanthra[2,1,9-def;6,5,10-d'e'f']diisoquinoline-1,3,8,10-tetraone (3): 9-(1-Hexylheptyl)-2-benzopyrano[6',5',4':10,5,6]anthra[2,1,9-def]isoquinoline-1,3,8,10-tetraone (0.15 g, 0.26 mmol),^[34] formanilide (63 mg, 0.52 mmol), and imidazole (5.0 g) were heated at 150 °C for 3 h and then allowed to cool. While still warm, the solution was treated with aqueous HCl (2 M, 50 mL). The precipitate was collected by vacuum filtration, dried at 110 °C, purified by column separation (silica gel, chloroform) and finally precipitated with methanol from chloroform and dried at 110 °C. Yield: 0.13 g (77%) red solid. M.p. > 250 °C. R_f value (silica gel, chloroform) = 0.25; 1H NMR (600 MHz, $CDCl_3$, 25 °C, the Supporting Information, Figure S3): δ = 0.82 (t, $^3J(H,H)$ = 6.9 Hz, 6H, $2 \times CH_3$), 1.17–1.37 (m, 16H, $8 \times CH_2$), 1.82–1.90 (m, 2H, $\beta-CH_2$), 2.19–2.29 (m, 2H, $\beta-CH_2$), 5.15–5.21 (m, 1H, N-CH), 7.33–7.36 (m, 2H, $2 \times CH_{arom.}$), 7.49–7.52 (m, 1H, $CH_{arom.}$), 7.56–7.59 (m, 2H, $2 \times CH_{arom.}$), 8.62–8.75 ppm (m, 8H, $8 \times CH_{perylene}$). ^{13}C NMR (150 MHz, $CDCl_3$, 25 °C, Figure S4): δ = 14.0, 22.6, 26.9, 29.2, 29.7, 31.7, 32.4, 54.8, 123.1, 123.3, 126.4, 126.7, 128.6, 128.9, 129.5, 129.8, 129.8, 131.1, 131.8, 134.3, 135.1, 163.6 ppm; IR (ATR): $\tilde{\nu}$ = 2921.0 (w), 1695.9 (m), 1652.9 (s), 1592.0 (m), 1575.9 (m), 1505.3 (w), 1433.2 (w), 1403.4 (m), 1341.8 (s), 1252.9 (m), 1177.2 (m), 1027.9 (w), 966.0 (w), 860.0 (w), 847.1 (w), 837.6 (w), 809.1 (s), 744.1 (s), 698.9 (m), 688.1 (w), 668.0 cm^{-1} (w); UV/Vis ($CHCl_3$): λ_{max} (ϵ) = 459.2 (20400), 490.4 (54700), 527.0 nm (90500); fluorescence ($CHCl_3$): λ_{max} (I_{rel}) = 496.4 (1.00), 538.7 (0.48), 588.4 nm (0.11); fluorescence quantum yield ($CHCl_3$, λ_{exc} = 490 nm, $E_{490\text{ nm}/1\text{ cm}}$ = 0.0127, reference 2,9-bis-(1-hexylheptyl)anthra[2,1,9-def;6,5,10-d'e'f']diisoquinoline-1,3,8,10-(2H,9H)-tetraone RN110590-8-6 with Φ = 1.00): 1.00; MS (DEP/El): m/z (%): 648.3 (17) [M^+], 443.2 (32), 181.6 (34); HRMS: m/z calcd for $C_{45}H_{40}N_2O_4$ 648.2988; found: 648.2980, Δ = -0.0008; elemental analysis calcd (%) for $C_{45}H_{40}N_2O_4$ (648.3): C 79.60, H 6.21, N 4.32; found: C 79.43, H 6.24, N 4.27.

Synthesis of MIL-101(Al)-NH₂: MIL-101(Al)-NH₂ was synthesized following a slightly modified procedure of Kapteijn and co-workers.^[22] The reaction was carried out in a 50 mL glass reactor. Aluminum(III) chloride hexahydrate (510 mg, 2.11 mmol) and 2-aminoterephthalic acid (560 mg, 3.09 mmol) were dissolved in *N,N*-dimethylformamide (DMF, 30 mL) in an ultrasonic bath. The sealed glass reactor was kept for 72 h in a preheated oven at 403 K. The resulting yellow powder was filtered under vacuum and washed with acetone. To remove the organic species trapped within the pores, the sample was extracted in ethanol heated at reflux for 8 h. Finally, the sample was dried in vacuo.

Synthesis of MIL-101(Al)-NH₂-perylene samples: The solvothermal synthesis of MIL-101(Al)-NH₂-perylene samples was carried out in a 50 mL glass reactor. Aluminum(III) chloride hexahydrate (510 mg, 2.11 mmol), 2-aminoterephthalic acid (560 mg, 3.09 mmol) and different amounts of 2-[9-(1-hexylheptyl)-1,3,8,10-tetraoxo-3,8,9,10-tetrahydro-1H-anthra[2,1,9-def;6,5,10-d'e'f']diisoquinolin-2-yl]terephthalic acid **2** (for MIL-101(Al)-NH₂-perylene40: 550 mg, 0.075 mmol; for MIL-101(Al)-NH₂-perylene200: 110 mg, 0.015 mmol; for MIL-101(Al)-NH₂-perylene1100: 20 mg, 0.003 mmol) were dissolved in DMF (30 mL) in an ultrasonic bath. The sealed glass reactor was kept for 72 h in a preheated oven at

403 K. The resulting red powder was filtered under vacuum and washed with acetone. To remove the organic species trapped within the pores, the samples were extracted in ethanol heated at reflux for 8 h and then purified by Soxhlet extraction in chloroform for 8 h. Finally, the sample was dried in vacuo.

Synthesis of MIL-101(Al)-NH₂-peryleneRef sample: The solvothermal synthesis of MIL-101(Al)-NH₂-peryleneRef sample was carried out in a 50 mL glass reactor, aluminum(III) chloride hexahydrate (510 mg, 2.11 mmol), 2-aminoterephthalic acid (560 mg, 3.09 mmol) and different amounts of (1-hexylheptyl)-9-phenylanthra[2,1,9-def;6,5,10-d'e'f']diisoquinoline-1,3,8,10-tetraone **3** (49 mg, 0.075 mmol) were dissolved in DMF (30 mL) in an ultrasonic bath. The sealed glass reactor was kept for 72 h in a preheated oven at 403 K. The resulting red powder was filtered under vacuum and washed with acetone. To remove organic species trapped within the pores and not bounded dye **3**, the sample was extracted in ethanol heated at reflux for 8 h and then purified by Soxhlet extraction in chloroform for 8 h. Finally, the sample was dried in vacuo.

Postsynthetic modification of MIL-101(Al)-NH₂-perylene samples: MIL-101(Al)-NH₂-perylene samples were dispersed in acetic anhydride (1 mL/10 mg MOF) at 100 °C. After 10 min the sample was filtered immediately and washed three times with acetone. Finally, samples were dried in vacuo.

Digestion of MIL-101(Al)-NH₂-perylene samples: For digestion of the sample about 3 mg sample was added to a solution of 24 mg caesium fluoride in 450 μ L $[D_6]DMSO$ and 250 μ L D_2O . After vortex mixing, the suspension was sonicated for 5 min. After repeating this procedure once again the solution was transferred in a NMR tube. For determination of postfunctionalization yield integral of peak A of postfunctionalized 2-aminoterephthalic acid was divided by the sum of integral A and integral A' of 2-aminoterephthalic acid (see Figure S11, the Supporting Information, for proton denotation).

Acknowledgements

The authors are grateful for financial support from the Center for NanoScience Munich (CeNS) and for the support of Prof. Thomas Bein (LMU).

Keywords: dyes • fluorescence • metal–organic frameworks • NMR spectroscopy • synthetic methods

- [1] Theme Issue: Metal-Organic Frameworks, H.-C. Zhou, J. R. Long, O. M. Yaghi, *Chem. Rev.* **2012**, 112, 673–674.
- [2] Theme Issue: Metal-Organic Frameworks, H.-C. J. Zhou, S. Kitagawa, *Chem. Soc. Rev.* **2014**, 43, 5415–5418.
- [3] G. Férey, *Chem. Soc. Rev.* **2008**, 37, 191.
- [4] E. Kreno, K. Leong, O. K. Farha, M. Allendorf, R. P. Van Duyne, J. T. Hupp, *Chem. Rev.* **2012**, 112, 1105–1125.
- [5] A. Hulanicki, S. Glab, F. Ingman, *Pure Appl. Chem.* **1991**, 63, 1247–1250.
- [6] J. M. Küner, I. Klimant, C. Krause, H. Preu, W. Kunz, O. S. Wolfbeis, *Bioconjugate Chem.* **2001**, 12, 883.
- [7] M. D. Allendorf, C. A. Bauer, R. K. Bhadkta, R. J. T. Houka, *Chem. Soc. Rev.* **2009**, 38, 1330.
- [8] B. V. Harbuzaru, A. Corma, F. Rey, P. Atienzar, J. L. Jord, H. Garca, D. Ananias, L. D. Carlos, J. Rocha, *Angew. Chem. Int. Ed.* **2008**, 47, 1080; *Angew. Chem.* **2008**, 120, 1096.
- [9] B. V. Harbuzaru, A. Corma, F. Rey, J. L. Jord, D. Ananias, L. D. Carlos, J. Rocha, *Angew. Chem. Int. Ed.* **2009**, 48, 6476; *Angew. Chem.* **2009**, 121, 6598.

- [10] A. Modrow, D. Zargarani, R. Herges, N. Stock, *Dalton Trans.* **2012**, 41, 8690.
- [11] F. M. Hinterholzinger, S. Wuttke, P. Roy, T. Preuße, A. Schaate, P. Behrens, A. Godt, T. Bein, *Dalton Trans.* **2012**, 41, 3899.
- [12] K. M. L. Taylor-Pashow, J. D. Rocca, Z. Xie, S. Tran, W. Lin, *J. Am. Chem. Soc.* **2009**, 131, 14261–14263.
- [13] J. Aguilera-Sigalat, D. Bradshaw, *Chem. Commun.* **2014**, 50, 4711.
- [14] S. Wuttke, C. Dietl, F. M. Hinterholzinger, H. Hintz, H. Langhals, T. Bein, *Chem. Commun.* **2014**, 50, 3599.
- [15] Y. Takashima, V. Martínez Martínez, S. Furukawa, M. Kondo, S. Shimomura, H. Uehara, M. Nakahama, K. Sugimoto, S. Kitagawa, *Nat. Commun.* **2011**, 2, 168.
- [16] C. Y. Lee, O. K. Farha, B. J. Hong, A. A. Sarjeant, S. T. Nguyen, J. T. Hupp, *J. Am. Chem. Soc.* **2011**, 133, 15858.
- [17] Z. W. Wei, Z. Y. Gu, R. K. Arvapally, Y. P. Chen, R. N. McDougald, Jr., J. F. Ivy, A. A. Yakovenko, D. W. Feng, M. A. Omary, H. C. Zhou, *J. Am. Chem. Soc.* **2014**, 136, 8269–8276.
- [18] H. Deng, C. J. Doonan, H. Furukawa, R. B. Ferreira, J. Towne, C. B. Knobler, B. Wang, O. M. Yaghi, *Science* **2010**, 327, 846.
- [19] C. Wang, D. Liu, Z. Xie, W. Lin, *Inorg. Chem.* **2014**, 53, 1331.
- [20] W. Kleist, F. Jutz, M. Maciejewski, A. Baiker, *Eur. J. Inorg. Chem.* **2009**, 3552.
- [21] S. Marx, W. Kleist, J. Huang, M. Maciejewski, A. Baiker, *Dalton Trans.* **2010**, 39, 3795.
- [22] F. M. Hinterholzinger, B. Rühle, S. Wuttke, K. Karaghiosoff, T. Bein, *Sci. Rep.* **2013**, 2, 2562.
- [23] G. Férey, C. Mellot-Draznieks, C. Serre, F. Millange, J. Dutour, S. Surblé, I. Margiolaki, *Science* **2005**, 309, 2040–2042.
- [24] P. Serra-Crespo, E. V. Ramos-Fernandez, J. Gascon, F. Kapteijn, *Chem. Mater.* **2011**, 23, 2565.
- [25] M. Hartmann, M. Fischer, *Microporous Mesoporous Mater.* **2012**, 164, 38.
- [26] H. Hintz, S. Wuttke, *Chem. Commun.* **2014**, 50, 11472–11475.
- [27] H. Langhals, *Helv. Chim. Acta* **2005**, 88, 1309.
- [28] H. Langhals, *J. Electr. Electron. Syst.* **2014**, 3, 125.
- [29] *Fluorescence Spectroscopy. New Methods and Applications* (Ed.: O. S. Wolfbeis), Springer, Berlin, **1993**, p. 310.
- [30] *Fluorescence Sensors and Biosensors* (Ed.: R. B. Thompson), CRC, Boca Raton, **2006**; *Chem. Abstr.* **2006**, 145, 23798.
- [31] H. Langhals, W. Jona, *Eur. J. Org. Chem.* **1998**, 847.
- [32] X. Kong, H. Deng, F. Yan, J. Kim, J. A. Swisher, B. Smit, O. M. Yaghi, J. A. Reimer, *Science* **2013**, 341, 882.
- [33] H. Langhals, W. Jona, *Chem. Eur. J.* **1998**, 4, 2110.
- [34] S. M. Cohen, *Chem. Rev.* **2012**, 112, 970.
- [35] H. Hintz, S. Wuttke, *Chem. Mater.* **2014**, 26, 6722.
- [36] H. Langhals, T. Pust, *Green Sustainable Chem.* **2011**, 1, 1.
- [37] H. Langhals, R. Ismael, *Eur. J. Org. Chem.* **1998**, 1915.
- [38] H. Kaiser, J. Lindner, H. Langhals, *Chem. Ber.* **1991**, 124, 529.
- [39] J.-P. Amoureux, C. Fernandez, S. Steuernagel, *J. Magn. Reson. Ser. A* **1996**, 123, 116–118.
- [40] B. Herreros, A. W. Metz, G. S. Harbison, *Solid State Nucl. Magn. Reson.* **2000**, 16, 141–150.

Received: November 20, 2014

Published online on June 2, 2015